Available online at www.sciencedirect.com

ScienceDirect

Current Opinion in Chemical Engineering

Review

Metal–organic framework–based heterojunctions for photocatalysis

Ran Tai[1,*], Runjie Wu[1,*], Mingzhu Zhang[2], Jie Yuan[3], John Tressel[4], Yao Tang[1], Qiang Wang[1] and Shaowei Chen[4]

Metal–organic frameworks (MOFs) have attracted much attention in photocatalysis due to their unique molecular architecture and diverse composition, where the performance can be effectively enhanced by the construction of heterojunctions. In this review, we summarize the recent progress of MOF-based photocatalysts with traditional heterojunctions (e.g. type I, type II, and p-n type) as well as Z- and S-scheme and even multicomponent heterojunctions, where the advantages and disadvantages of these heterojunctions in their photocatalytic applications toward environmental remediation and energy conversion are critically discussed. The review is concluded with a perspective for the further development of high-performance photocatalysts based on deliberate heterojunction engineering of MOF materials.

Addresses
[1] Laboratory for Micro-sized Functional Materials & College of Elementary Education and Department of Chemistry, Capital Normal University, Beijing 100048, China
[2] School of Mechanical and Electrical Engineering, Beijing Polytechnic College, Beijing 100048, China
[3] State Key Laboratory of Photocatalysis on Energy and Environment, Fuzhou University, Fuzhou, Fujian 350116, China
[4] Department of Chemistry and Biochemistry, University of California, 1156 High Street, Santa Cruz, California 95064, USA

Corresponding authors: Wang, Qiang (qwchem@gmail.com), Chen, Shaowei (shaowei@ucsc.edu)
[*] These authors contributed equally to the work.

Current Opinion in Chemical Engineering 2024, **45**:101033

This review comes from a themed issue on **Scheme Photocatalysis**

Edited by **Fang Deng**

Available online xxxx

https://doi.org/10.1016/j.coche.2024.101033

Introduction

Photocatalysis has been used extensively as an environmentally friendly technology in the fields of sustainable energy conversion and environmental remediation, where the rational design of high-performance catalysts represents a critical first step [1–3]. Toward this end, metal–organic frameworks (MOFs), a class of porous framework materials, have been attracting a great deal of attention, mainly because the materials structure can be readily tailored and controlled with atomic precision, and the metal nodes and organic linkages can be deliberately functionalized [4]. The resulting framework structure leads to spatial separation of the active sites and minimizes their aggregation and inactivation. Indeed, MOFs have been used as photocatalysts for a range of applications due to a moderate band gap; yet the performance is typically rather limited thanks to a high recombination rate of photogenerated carriers and slow charge migration [5]. Within this context, a number of strategies have been developed to engineer the MOF structure for enhanced performance, such as heteroatom doping, defect engineering, and construction of heterostructures [6,7]. Among these, heterojunctions have been found to facilitate charge carrier separation and transport, effectively improving the photocatalytic activity. Such unique structures can be obtained by exploiting MOFs as a functional scaffold for the growth of other materials, where the different energy band structures of the structural components lead to ready manipulation of the charge transfer dynamics [8,9].

Thus far, a variety of heterojunctions have been reported, which include the traditional type I (straddling gap), type II (staggered gap), and p-n type [10], as well as the new Z-scheme [11] and S-scheme heterojunctions [12]. Whereas traditional heterojunctions have been found to effectively suppress carrier recombination, the performance has remained nonideal due to limited redox potentials. Such issues can be mitigated by Z-scheme and S-scheme heterojunctions [13], where the former can possess favorable thermodynamic charge transfer pathways, while the energy band bending and built-in electric field in the latter are known to improve the carrier separation and transmission efficiency [14,15]. Notably, the photocatalytic performance can be manipulated by a range of experimental parameters, such as heterojunction size, composition, microenvironment, and structural stability, among others [16,17].

In this review, we will summarize the latest progress in the construction and engineering of MOF-based heterojunctions, with a focus on the mechanistic understanding of the photocatalytic activity toward important reactions in environmental remediation and sustainable energy conversion. We conclude the review with a perspective for the further development of MOF heterojunction-based photocatalysts.

Metal–organic framework materials

Classification

MOFs are porous crystalline materials by self-assembly of multidentate organic ligands and inorganic metal ions or clusters through coordination bonds, van der Waals forces or hydrogen bonds [18]. Thus far, more than 20 000 MOF materials have been reported in the literature. According to the component units and synthesis conditions, MOF materials can be divided into four major categories: isoreticular MOFs (IRMOFs), zeolitic imidazolate frameworks (ZIFs), Materials of Institute Lavoisier frameworks (MILs), and porous and channel framework materials (Pocket-channel Frameworks [PCNs]). These materials are typically prepared by using solvothermal, hydrothermal, solvent volatilization, gas-phase thermal decomposition, templating, ultrasound-assisted, and microwave-radiation methods so as to obtain MOF materials with specific morphology, pore structure, and photocatalytic properties. IRMOFs consist mainly of a repeating network topology formed by $[Zn_4O_6]^+$ metal clusters bonded with carboxylic acid–-based organic ligands, displaying a large specific surface area, high porosity, and adjustable pore size [19]. Among them, IRMOF-1 (MOF-5, Figure 1a) [20] and IRMOF-3 [21] are the well-known examples. ZIFs are produced by self-assembly of Zn or Co ions bonded to the N sites of the imidazole (or imidazole derivatives) ring in a four-coordinate manner. ZIFs are known to exhibit structural diversity and easy to functionalize, with ZIF-8 (Figure 1b) [22] and ZIF-67 [23] being the most common and most synthesized ones. MILs are formed by the coordination of trivalent transition metal ions (such as Fe, Al, and Cr) to carboxylic acid ligands (e.g. terephthalic acid, trimesic acid, etc) and typically possess a high specific surface area and rich porosity. Among them, MIL-88A [24], MIL-100 (Figure 1c) [25], and MIL-101 [26] have been extensively studied and used in various fields. PCNs typically consist of metal centers, such as copper, zinc, iron, and zirconium, that are in coordination bonds with porphyrin ligands. Among these, tetrakis(4-carboxyphenyl)porphyrin is a popular one because of the excellent stability and diverse functions, for instance, PCN-*222* [27], PCN-*224* [28], and PCN-416 (Figure 1d) [29] that have found unique applications in sensing, photoelectrocatalysis, and others due to their large pores, good stability, and high density of catalytic active sites.

Coordination pillared-layer (CPL) materials represent another addition to the MOF family, consisting of a porous organic coordination polymer composed of six-coordinate metal nodes and neutral nitrogen-containing heterocyclic ligands. The synthesis is generally rather simple, and the material structures are flexible with adjustable pore size. CPL materials have therefore been utilized in the fields of gas adsorption and energy storage [30]. The well-known examples of CPLs are the UiO (Universitetet i Oslo) series (e.g. UiO-66 [31], Figure 1e), UiO-67, UiO-68 and UiO-69) that are composed of $[Zr_6O_4(OH)_4]$ coordinated to 12 terephthalic acid ligands forming a regular octahedral crystal structure. These materials feature unique structural characteristics, such as a relatively uniform size and strong stability, and have indeed found diverse applications.

Materials structures

A notable feature of MOF materials is their high specific surface area due to the unique pore structure [32]. This not only provides a large amount of void space for storing reaction substances but also facilitates the formation of abundant active site, leading to a high performance in adsorption and separation of reactive species [33]. The porosity of MOFs can be tailored by changing the types and feeds of organic ligands and metal nodes to meet the needs of different reactions (Figure 1f) [34]. For instance, MOFs with large pore sizes will be preferred for catalytic reactions that entail macromolecular reaction species. By adjusting the porosity, the adsorption and diffusion properties of MOFs can be further optimized, thereby further improving the efficiency and selectivity of catalytic reactions.

The structure and function of MOFs can be enriched by the incorporation of different functional groups, metal clusters, nanoparticles, etc. (Figure 1g) [35,36]. Structural engineering can also be achieved by postsynthesis processing, such as thermal treatment, solvent exchange, etc. [37]. This renders it possible to tailor the chemical and physical properties of the MOFs materials for specific applications.

Another important feature of MOFs is the controllable defects within the structural frameworks. These defects can be produced by careful control of the synthesis conditions and selection of the organic ligands and be exploited for the manipulation of the electronic band structure and charge transport dynamics. This may not only lead to the formation of new catalytic active sites but also serve as electronic traps to inhibit the recombination of

Figure 1

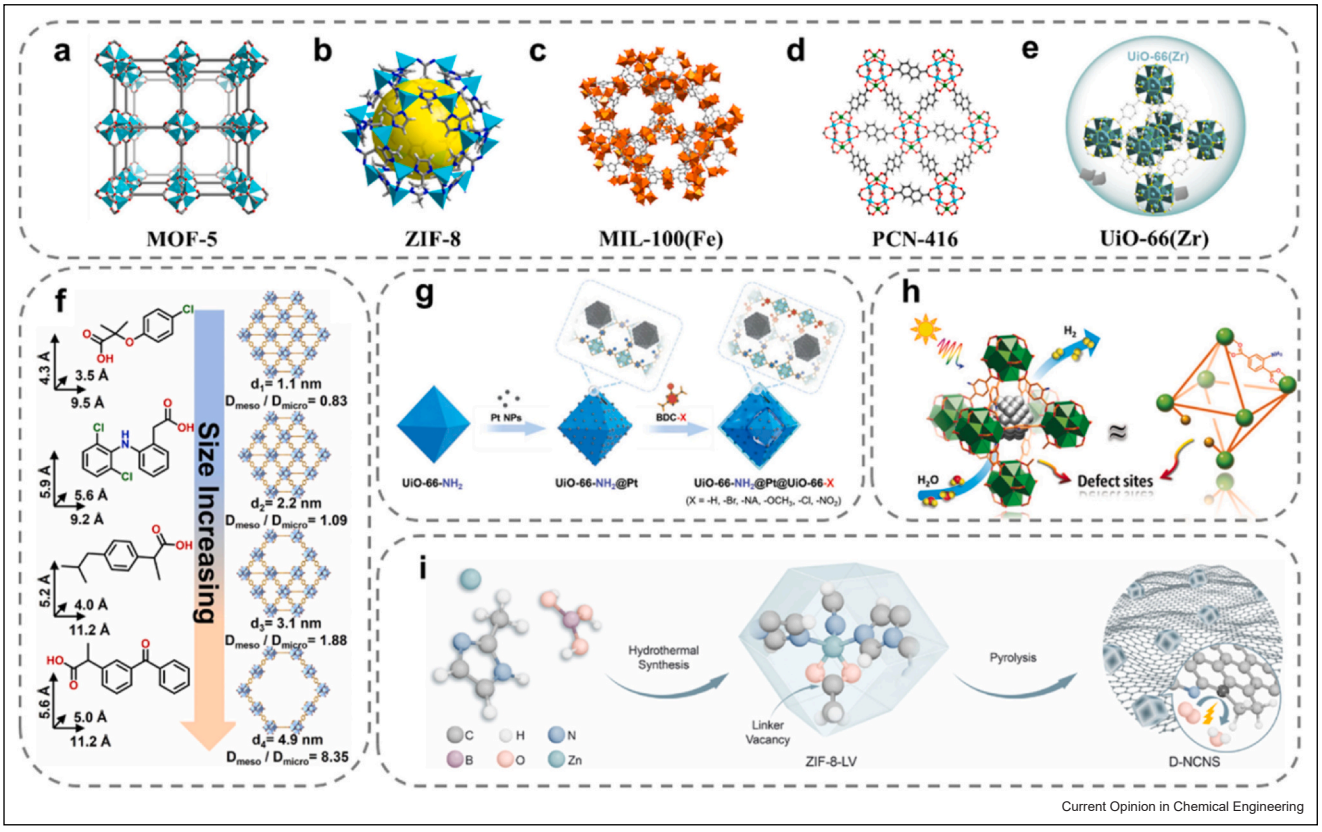

Structures of different types of MOFs: **(a)** MOF-5. Copyright 2023, American Chemical Society. **(b)** ZIF-8. Copyright 2022, Wiley Online Library. **(c)** MIL-100(Fe). Copyright 2023, American Chemical Society. **(d)** PCN-416. Copyright 2018, American Chemical Society. **(e)** UiO-66(Zr). Copyright 2021, American Chemical Society. **(f)** Schematic illustration of the increasing pore structure of synthesized UiO-66 via templated (modulator)-induced synthesis process and target representative pharmaceuticals and personal care products (PPCPs) with different molecular sizes. Copyright 2023, Elsevier. **(g)** Schematic illustration of the stepwise synthesis of sandwich-structured UiO-66-NH_2@Pt@UiO-66-X (X = H, Br, NA, OCH_3, Cl, NO_2) composites. Copyright 2023, Wiley Online Library. **(h)** Photocatalytic hydrogen production over Pt@UiO-66-NH_2-X with structural defects. Copyright 2019, Wiley Online Library. **(i)** Scheme of the synthesis route to D-NCNS electrocatalysts. Copyright 2023, Elsevier.
(a) Adapted with permission from Ref. [15]. **(b)** Adapted with permission from Ref. [17]. **(c)** Adapted with permission from Ref. [20]. **(d)** Adapted with permission from Ref. [24]. **(e)** Adapted with permission from Ref. [26]. **(f)** Adapted with permission from Ref. [29]. **(g)** Adapted with permission from Ref. [30]. **(h)** Adapted with permission from Ref. [33]. **(i)** Adapted with permission from Ref. [34].

carriers, thereby improving the efficiency and selectivity of the photocatalytic performance (Figure 1h–i) [38,39].

Heterojunction engineering

Thus far, a series of MOF-based heterojunctions have been designed and constructed for photocatalysis, involving different interfacial charge–transfer mechanisms [40]. In this section, the design principles and recent progress of four types of MOF-based heterojunctions and their impacts on the photocatalytic activity will be discussed: (1) traditional heterojunctions, (2) Z-scheme heterojunctions, (3) S-scheme heterojunctions, and (4) multicomponent heterojunctions.

Traditional heterojunctions

In the traditional type I heterojunctions, the conduction band minimum and valence band maximum of the semiconductor with a lower bandgap are straddled within those of the semiconductor with a larger bandgap [41]. Upon photoirradiation, both semiconductors will be excited; yet the photogenerated electrons and holes will migrate to the conduction band and valence band of the lower-bandgap material, respectively, facilitating separation of the charge carriers. For instance, Wu et al. [42] loaded Fe atoms into the organic ligands of Fe-MOF-525 and constructed a CdS/Fe-MOF-525 type I photocatalyst by physical ball milling (Figure 2a), where photogenerated electrons and holes effectively transferred from CdS to Fe-MOF-525. In comparison to pure Fe-MOF-525, the addition of CdS helped stabilize the Fe active sites and improved the photocatalytic activity toward hydrogen evolution, with a hydrogen evolution rate (3638.6 μmol g^{-1} h^{-1}) that was 7.2 and 2.3 times higher than those of Fe-MOF-525 and CdS, respectively.

Figure 2

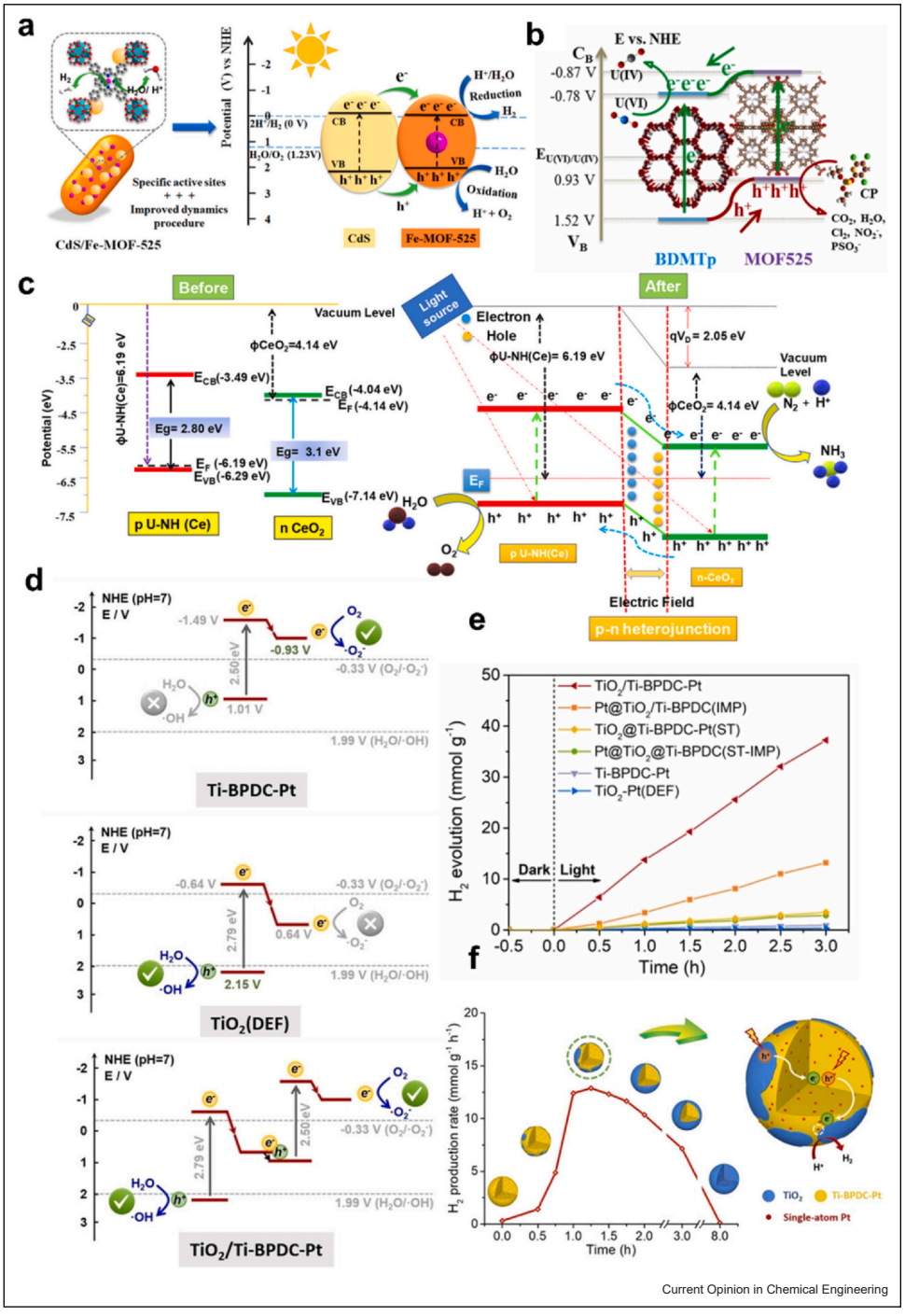

Schematics of different types of MOF-based heterojunctions: **(a)** Photocatalytic mechanism of CdS/Fe-MOF-525. Copyright 2023, American Chemical Society. **(b)** Schematic diagram of photocatalytic removal of U(VI) and CP by MOF525@BDMTp. Copyright 2023, Elsevier. **(c)** Schematic diagram presenting the mechanism of NH_3 formation and oxygen evolution over the formed CeO_2/UNH (Ce) p-n Heterojunction (rod@sheet). Copyright 2021, American Chemistry Society. **(d)** Schematic band structures of Ti-BPDC-Pt, TiO_2(DEF), and TiO_2/Ti-BPDC-Pt. **(e)** H_2 evolution as a function of the reaction time of catalysts under irradiation at $\lambda > 420$ nm. **(f)** High activity is confirmed due to the efficient charge separation promoted by the heterojunction and the selective location of Pt single-atomic cocatalysts on the electron-enriched domain of the heterojunction. Copyright 2023, Wiley. **(a)** Adapted with permission from Ref. [37]. **(b)** Adapted with permission from Ref. [38]. **(c)** Adapted with permission from Ref. [40]. **(d)** Adapted with permission from Ref. [42].

However, the spatial separation of carriers in traditional type I heterojunctions is nonideal, and the redox capacity of carriers is limited, which hinders the overall photocatalytic performance.

In type II heterojunctions, the valence and conduction bands of the two semiconductors (A and B) are arranged in a staggered manner [41]. Photogenerated electrons migrate from the higher-energy conduction band of A to the lower-energy conduction band of B and become enriched on B, whereas holes migrate in the opposite direction from the valence band of B to that of A and become enriched on A. Consequently, photogenerated electrons and holes are effectively separated. For example, as shown in Figure 2b, Liu et al. [43] synthesized a bifunctional MOF525@BDMTp composite with a MOF core and a covalent organic framework (COF) shell bridged covalently. The introduction of MOF525 increased the photo absorption range, and the introduction of BDMTp COF increased the active sites. Notably, the type II heterostructure formed by the combination of the two endowed the composite with 'electronic sponge' type charge storage and transport. Due to band bending and internal electric field, the electrons on MOF525 conduction band transferred to BDMTp and accumulated at the N- and O-sites, which facilitated the adsorption and reduction of U(VI) on BDMTp and oxidation of chlorpyrifos on MOF525. Under UV–vis photoirradiation for 4 hours, the U(VI) removal rate was found to be 625.0 $mg\,g^{-1}$ and the chlorpyrifos removal rate over 94.0%.

The disadvantages of type II heterojunctions in photocatalysis are mainly manifested in the high recombination rate of photogenerated electrons and holes that limits the photocatalytic efficiency, and an increase in defects at the interface and a complicated preparation process that hinder the practical application and large-scale production. There is also a type III heterojunction, in which the valence band of one semiconductor is even higher than the conduction band of the other, such that the energy bands of these two semiconductors are arranged discontinuously. Therefore, there is no migration between electrons and holes at the interface, and this type of heterojunctions can not improve the photocatalytic performance.

When p-type and n-type semiconductors are in intimate contact, p-n heterojunctions are formed at the interface, which constitute another member of the traditional heterojunctions. For p-n heterojunctions, a depletion layer and a built-in electric field are produced due to the difference of the Fermi levels [44]. When a p-n heterojunction is exposed to photoirradiation, photogenerated carriers are generated in the respective semiconductors. Due to the built-in electric field, electrons will migrate from the p-type semiconductor to the n-type semiconductor, and holes will migrate in the opposite direction, thus achieving effective separation of the photogenerated carriers. For instance, Sriram et al. [45] constructed a p-n heterojunction between rod-shaped Ce-MOF-NH_2 (UNH (Ce)) and oxygen-vacancy-rich sheet-like CeO_2 through a hydrothermal method (Figure 2c), where electrons were found to transfer from the n-type CeO_2 with a higher Fermi level to the p-type UNH (Ce) with a lower Fermi level, and holes migrated in the opposite direction until the Fermi levels of the two reached an equilibrium. This charge transfer enriched negative charges on UNH (Ce) and positive charges on the CeO_2 side of the interface, generating a built-in electric field from CeO_2 to UNH (Ce) that effectively increased the carrier separation efficiency. At the same time, the presence of Ce^{3+} and oxygen vacancies promoted the adsorption and activation of N_2, and the ((1:1) CeO_2/UNH (Ce)) sample showed an excellent N_2 reduction and O_2 release rate of 47.55 μmol L^{-1}·h^{-1} and 370.18 μmol h370.18 μmol·h^{-1}, with the apparent conversion efficiencies of 0.33% and 8.5%, respectively. It is worth noting that while the p-n junctions are a specific type of semiconductor heterojunctions, the formation of other heterojunctions may implicate p-n junction–related concepts, especially with regard to charge distribution and potential difference.

Z-scheme heterojunctions

Z-scheme heterojunctions possess unique advantages over conventional type I, type II, and p-n heterojunctions in optoelectronic devices, as their structural design improves the interfacial charge separation efficiency, reduces the electron complex loss, and expands the spectral response range, thus significantly improving the device performance. In a Z-scheme heterojunction, if the Fermi level of semiconductor A is higher than that of semiconductor B, when the two semiconductors come into contact, electrons will migrate from A to B until the Fermi levels of the two semiconductors reach an equilibrium, generating an internal electric field at the interface in the direction of A to B [46]. Meanwhile, the energy band of A will bend upward at the interface, while the energy band of B will bend downward. Upon photoirradiation, the electrons in the conduction band of semiconductor B and the holes in the valence band of semiconductor A will recombine at the interface, causing the electrons and ions with strong reducing and oxidizing abilities in the heterojunction to recombine. As shown in Figure 2d–f, He et al. [47] anchored high-density Pt single-atom cocatalysts on a Ti-BPDC MOF, and pyrolysis of the resulting Ti-BPDC-Pt at 400°C for 12 hours produced a Z-scheme heterojunction of defect-rich TiO_2/Ti-BPDC-Pt. Upon photoirradiation, the electrons excited to the conduction band of TiO_2 migrated to the defect levels formed by oxygen vacancies and recombined with holes generated on the valence band of Ti-BPDC-Pt. Electrochemical and spectroscopic

measurements, in conjunction with density functional theory calculations, showed that with the formation of the heterojunction, electron transfer occurred from Ti-BPDC-Pt (which possessed a higher Fermi level) to the TiO_2 (DEF) surface until the Fermi level was aligned. This led to the formation of an electron depletion region and electron accumulation region at the heterojunction interface between Ti-BPDC-Pt and TiO_2 (DEF), where the difference of charge density between the two phases produced an internal electric field directed from the former to the latter at the interface, as well as upward bending of the Ti-BPDC-Pt energy band and downward bending of that of TiO_2 (DEF). Therefore, the resulting heterojunction composites exhibited a remarkable performance toward photocatalytic hydrogen evolution at a rate of 12.4 mmol g^{-1} h^{-1} with an apparent quantum yield of 19.17%.

Nevertheless, there are intrinsic disadvantages of Z-scheme heterojunctions in photocatalysis, such as complex preparation processes, high costs, and high requirements for material matching. Meanwhile, there may be defects at the interface, which can impact the charge transfer efficiency, and limit the feasibility in large-scale applications.

S-scheme heterojunctions

S-scheme heterojunctions, first proposed by Yu et al. in 2019 [48], represent a new addition consisting of two n-type semiconductors that feature an 'S' shape transfer path of photogenerated carriers at the interface and possess a high redox capacity [49]. In comparison to oxidation photocatalysts, reduction photocatalysts typically exhibit a higher work function and lower Fermi level. When reduction photocatalysts come into contact with oxidation photocatalysts, electron transfer occurs from the former to the latter, forming regions of different charge density and hence a built-in electric field. This causes the energy bands to bend in different directions, and the formation of an S-shaped heterojunction in a staggered manner. The built-in electric field, energy band bending, and electrostatic interaction at the interface greatly facilitate the combination of electrons on the oxidation photocatalysts (which feature a weak reduction potential) and holes on the reduction photocatalysts (which feature a weak oxidation potential), and hence retain the stronger redox potential. In comparison to Z-scheme heterojunctions, S-scheme heterojunctions are advantageous in that they exhibit a simpler structure and are easier to prepare and control. In addition, the charge separation efficiency of S-scheme heterojunctions is usually higher, which helps improve the performance of the optoelectronic devices.

Recently, S-scheme heterojunctions have also been extended to p-type and n-type semiconductors, as well as MOFs, which are mostly n-type semiconductors with a narrow band gap [50]. Yet, studies of S-scheme heterojunctions have remained scarce thus far, and doping and cocatalyst modification have been proposed to enhance the heterojunction efficiency [51]. Nevertheless, despite an excellent theoretical performance, it remains difficult to experimentally identify/confirm the S-scheme heterojunctions. For instance, Xu et al. [12] synthesized CeO_2/Ce-MOF homologous S-scheme heterojunction photocatalysts through a simple hydrothermal method for the elimination of acetaldehyde. As shown in Figure 3a–f, the authors used Kelvin probe force microscopy (KPFM) to study the change of surface potential of CeO_2/Ce-MOF heterojunctions before and after photo illumination, which clearly identified electron-accepting CeO_2 (point A) and electron-donating Ce-MOF (point B), and surface photovoltage measurements showed that photogenerated electrons were transferred from Ce-MOF to CeO_2, confirming the formation of an S-scheme heterojunction. The relaxation path and dissociation process of photogenerated charges were also analyzed through femtosecond transient absorption spectroscopy (fs-TA) measurements (Figure 3g–j). The transfer and recombination of electron–hole pairs further supported the formation of an S-scheme heterojunction (Figure 3k), which facilitated the separation of photogenerated carriers and effectively impeded their recombination, leading to a high performance toward the photocatalytic elimination of organic pollutants like acetaldehyde.

Multicomponent heterojunctions

Multicomponent heterojunctions have also been reported for enhanced photocatalysis. For instance, Yu et al. [52] successfully prepared Ag_3PO_4/MOF-In_2S_3/Bi_2S_3 double Z-scheme heterojunctions, which showed a high photocatalytic activity toward the degradation of antibiotic residues of ofloxacin. In another study, Yu et al. [53] prepared Ni-MOF/g-C_3N_4/CdS quaternary composites that contained type I, type II and S-scheme heterojunctions, forming a closed loop for electron migration, which led to a remarkable rate of photocatalytic hydrogen evolution (17.844 mmol g^{-1} h^{-1}) without precious metal-based cocatalysts.

In general, the preparation of multicomponent heterojunctions involves complex procedures, and the photocatalytic performance may be compromised by the limited stability of the composites. Thus, extensive research efforts are being devoted to mitigation of these issues because of their high potential in specific applications.

Figure 3

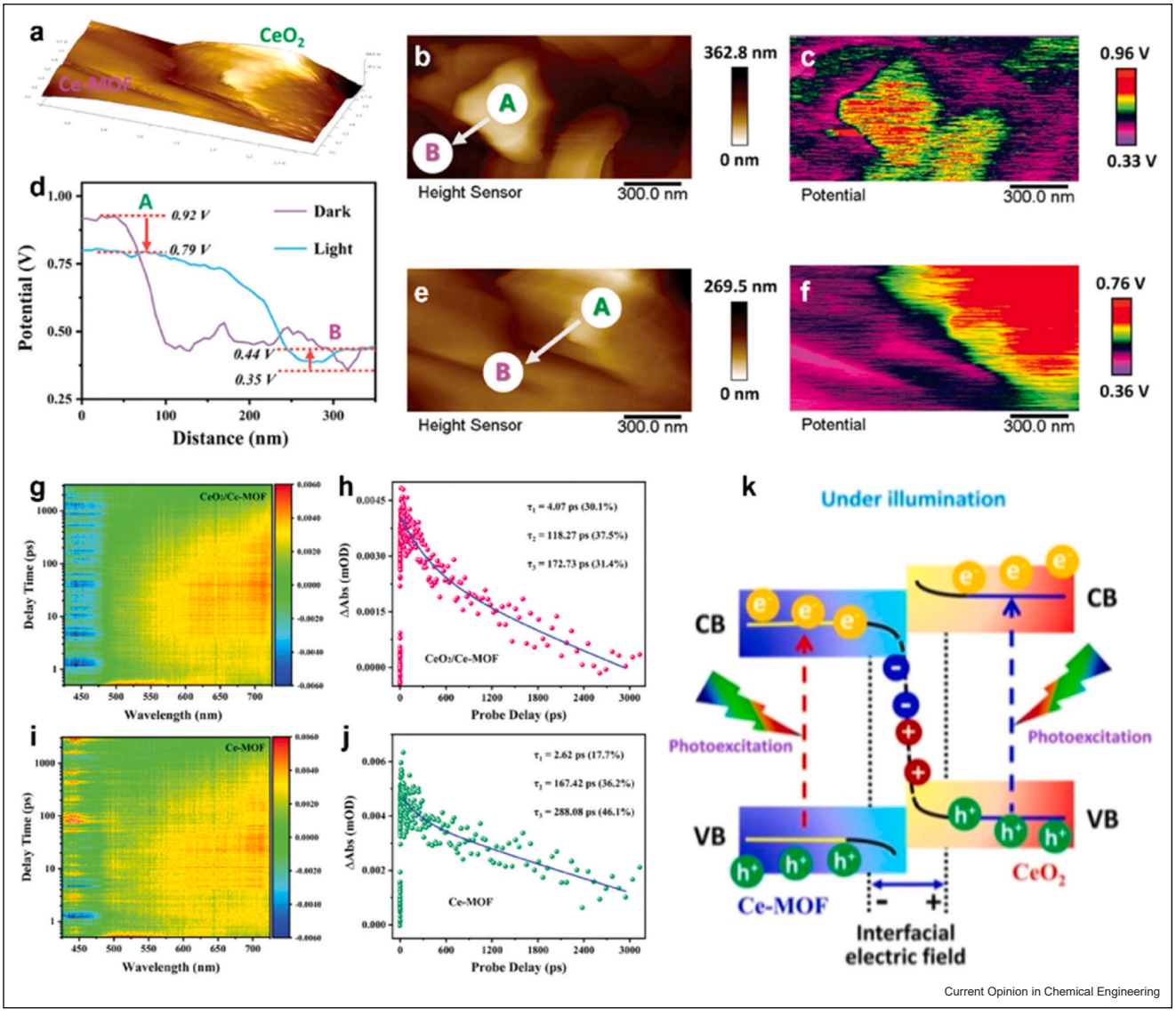

S-scheme heterojunction: **(a)** KPFM image of CeO_2/Ce-MOF photocatalyst. The corresponding surface potential distribution of CeO_2/Ce-MOF (b,c) in the dark and **(e,f)** under light irradiation. **(d)** Line-scanning surface potentials from CeO_2 (point A) and Ce-MOF (point B). Time-wavelength-dependent transient absorption (TA) color maps (pumped at 360 nm) and TA decay kinetics probed at 650 nm: **(g,h)** CeO_2/Ce-MOF and **(i,j)** Ce-MOF. **(k)** Band potentials and charge separation of CeO_2 and Ce-MOF, respectively.
Reproduced with permission from Ref. [9]. Copyright 2023, Wiley Online Library.

Conclusion and outlook

MOF-based heterojunctions have found diverse applications as effective photocatalysts in various fields, in particular, environmental remediation and sustainable energy technologies. Despite the progress in recent years, key challenges remain; in particular, the inherent complexity of the material structure poses significant challenges in unraveling the photocatalytic mechanisms. In addition, hindered by factors such as low light conversion efficiency and poor thermal stability, such photocatalysts have been far away from practical applications. Thus, further research is strongly desired to mitigate these critical issues, as summarized below.

(a) Rational design of MOF scaffolds. Development of universally applicable MOF materials with an optimal arrangement of structural units and enhanced nanoscale architectures will be an important first step toward the construction of MOF-based heterojunctions, such that the material's band structure

can be deliberately modulated to optimize the photocatalytic performance. This calls for the development of effective synthetic protocols.

(b) In-depth structural characterization. Unambiguous validation of the heterojuction structure plays a crucial role in the mechanistic correlation with the photocatalytic activity. This is of particular importance when restructuring occurs during the photocatalytic reactions. The issue can be effectively addressed by the development of *in situ*/operando microscopy and spectroscopy techniques to unravel the structural dynamics.

(c) Computational studies. The combination of theoretical calculations and experimental studies has been known to significantly advance our understanding of the photocatalytic mechanisms of MOF heterojunctions and is anticipated to continue playing a key role in future studies focusing on the temporal and spatial changes of photogenerated charges in MOF photocatalysis. Additionally, the significant potential of artificial intelligence (AI) and machine learning (ML) can also be exploited for the rationale design of heterojunction materials. Specifically, ML algorithms can be utilized for rapid screening of suitable MOF candidates, and AI models can be constructed to design MOF heterojunctions based on the band structures of different MOFs and the heterojunction types required for specific applications.

Data Availability

Data will be made available on request.

Declaration of Competing Interest

The authors declare that they have no known competing financial interests or personal relationships that could have appeared to influence the work reported in this paper.

Acknowledgements

R.T. and R.W. contributed equally to this work. This work was supported by the National Natural Science Foundation of China (52372212 and 21471103). S.W.C. thanks the National Science Foundation for partial support of the work (CHE-2003685).

References and recommended reading

Papers of particular interest, published within the period of review, have been highlighted as:

- • of special interest
- •• of outstanding interest

1. Wu YY, Ji HD, Liu QM, Sun ZY, Li PS, Ding PR, Guo M, Yi XH, Xu WL, Wang CC, Gao S, Wang Q, Liu W, Chen SW: **Visible light photocatalytic degradation of sulfanilamide enhanced by Mo doping of BiOBr nanoflowers**. *J Hazard Mater* 2022, **424**:127563.

2. Ding PR, Ji HD, Li PS, Liu QM, Wu YY, Guo M, Zhou ZA, Gao S, Xu WL, Liu W, Wang Q, Chen SW: **Visible-light degradation of antibiotics catalyzed by titania/zirconia/graphitic carbon nitride ternary nanocomposites: a combined experimental and theoretical study**. *Appl Catal B Environ* 2022, **300**:120633.

3. Liu JL, Zhang KT, Shang RR, Zhang H, Shen JH, Liu H, Tressel J, Bao Y, Hui AP, Xie HJ, Chen SW: **Theory-guided doping of LaCoO nanoparticles for enhanced antimicrobial performance**. *Chem Eng J* 2023, **464**:142710.

4. Tahir M, Ajiwokewu B, Bankole AA, Ismail O, Al-Amodi H, Kumar N: **MOF based composites with engineering aspects and morphological developments for photocatalytic CO_2 reduction and hydrogen production: a comprehensive review**. *J Environ Chem Eng* 2023, **11**:109408.

5. • Qian ZP, Zhang R, Xiao Y, Huang HW, Sun Y, Chen Y, Ma TY, Sun XD: **Trace to the source: self-tuning of MOF photocatalysts**. *Adv Energy Mater* 2023, **13**:2300086.
The authors summarize the strategies for the self-tunning of MOF photocatalysts within the context of component manipulation, structural defect, and crystal engineering. The implication in a wide range of application is also discussed, such as water splitting, CO_2/N_2 reduction, and environmental remediation.

6. Chen D, Ji X, Zhou X, Sun Q, Xu S, Mao L, Guo Z, Guan J, Li T-T, Qian J: **MOF-on-MOF-derived hollow FeNi3/N-doped carbon nanorods for efficient oxygen evolution**. *Chem Eng J* 2023, **470**:144418.

7. Li S, Han W, An Q-F, Yong K-T, Yin M-J: **Defect engineering of MOF-based membrane for gas separation**. *Adv Funct Mater* 2023, **33**:2303447.

8. Yuan L, Zhang CQ, Zou YY, Bao T, Wang J, Tang C, Du AJ, Yu CZ, Liu C: **A S-scheme MOF-on-MOF heterostructure**. *Adv Funct Mater* 2023, **33**:2214627.

9. Zhang Q, Bolisetty S, Cao Y, Handschin S, Adamcik J, Peng Q, Mezzenga R: **Selective and efficient removal of fluoride from water: in situ engineered amyloid fibril/ZrO_2 hybrid membranes**. *Angew Chem Int Ed* 2019, **58**:6012-6016.

10. Zhang XS, Liu ZF, Shao BB, Wu T, Pan Y, Luo SH, He M, Ge L, Sun JW, Cheng CY, Huang J: **Construction of ZnInS/MOF-525 heterojunction system to enhance photocatalytic degradation of tetracycline**. *Environ Sci Pollut R* 2023, **30**:67647-67661.

11. Liu JH, Zhang BB, Huang ZY, Wang WY, Xi XG, Dong PY: **MOF-derived InO microrod-decorated MgInS nanosheets: Z-scheme heterojunction for efficient photocatalytic degradation of tetracycline**. *Langmuir* 2023, **39**:17458-17470.

12. •• Yang H, Jia L, Zhang QT, Yuan SS, Ohno T, Xu B: **Efficient exciton dissociation on ceria chelated cerium-based MOF isogenous S-scheme photocatalyst for acetaldehyde purification**. *Small* 2023, **20**:2308743.
S-type charge transfer mechanism between CeO_2 and Ce-MOF is confirmed by XPS and KPFM measurements. The results provide important guidance in the rational design of MOF heterojunction photocatalysts based on rare-earth elements.

13. Lin M, Chen H, Zhang ZZ, Wang XX: **Engineering interface structures for heterojunction photocatalysts**. *Phys Chem Chem Phys* 2023, **25**:4388-4407.

14. Sharma P, Kumar A, Dhiman P, Sharma G, Tessema Mola G, Stadler FJ: **Recent progress in photocatalytic applications of metal tungstates based Z-scheme and S-scheme heterojunctions**. *J Ind Eng Chem* 2024, **132**:1-21.

15. Song Y, Jian M, Qiao L, Zhao Z, Yang Y, Jiao T, Zhang Q: **Efficient removal and recovery of Ag from wastewater using charged polystyrene-polydopamine nanocoatings and their sustainable catalytic application in 4-nitrophenol reduction**. *Acs Appl Mater Inter* 2024, **16**:5834-5846.

16. Balapure A, Dutta J, Ganesan R: **Recent advances in semiconductor heterojunction: a detailed review of fundamentals of the photocatalysis, charge transfer mechanism, and materials**. *RSC Appl Interfaces* 2024, **1**:43-69.

17. Wang M, Fu M, Li J, Niu Y, Zhang Q, Sun Q: **New insight into polystyrene ion exchange resin for efficient cesium sequestration: the synergistic role of confined zirconium phosphate nanocrystalline**. *Chin Chem Lett* 2024, **35**:108442.

18. Chen C, Fei L, Wang B, Xu J, Li B, Shen LH, Lin H: **MOF-based photocatalytic membrane for water purification: a review**. *Small* 2024, **20**:2305066.

19. Cai MR, Liang WL, Wang KX, Yin DG, Fu TT, Zhu RY, Qu CH, Dong XX, Ni J, Yin XB: **Aperture modulation of isoreticular metal organic frameworks for targeted antitumor drug delivery**. *Acs Appl Mater Inter* 2022, **14**:36366-36378.

20. Li JH, Liu PX, Chen Y, Zhou JF, Li JW, Yang JF, Zhang DL, Li JP, Li LB: **A customized hydrophobic porous shell for MOF-5**. *J Am Chem Soc* 2023, **145**:19707-19714.

21. Zheng JZ, Pang KL, Liu X, Li SX, Song R, Liu YL, Tang ZY: **Integration and synergy of organic single crystals and metal-organic frameworks in core-shell heterostructures enables outstanding gas selectivity for detection**. *Adv Funct Mater* 2020, **30**:2005727.

22. Lee H, Chi WS, Lee MJ, Zhang K, Edhaim F, Rodriguez KM, DeWitt SJA, Smith ZP: **Network-nanostructured ZIF-8 to enable percolation for enhanced gas transport**. *Adv Funct Mater* 2022, **32**:2207775.

23. Villalgordo-Hernández D, Diaz-Perez MA, Balloi V, Lara-Angulo MA, Narciso J, Serrano-Ruiz JC, Ramos-Fernandez EV: **Post-synthetic ligand exchange as a route to improve the affinity of ZIF-67 towards CO_2**. *Chem Eng J* 2023, **476**:146846.

24. Zhang MM, Lu MZ, Qiu TZ, Wang Q, Chen ZX, Deng ML, Yang YT, Yang YN, Li W, Ling Y, Zhou YM: **Gelothermal synthesis of monodisperse MIL-88A nanoparticles with tunable sizes and metal centers for potential bioapplications**. *Small* 2023, **19**:2301894.

25. • Tofoni A, Tavani F, Vandone M, Braglia L, Borfecchia E, Ghigna P, Stoian DC, Grell T, Stolfi S, Colombo V, D'Angelo P: **Full spectroscopic characterization of the molecular oxygen-based methane to methanol conversion over open Fe(II) sites in a metal-organic framework**. *J Am Chem Soc* 2023, **145**:21040-21052.

The authors employ a wide range of advanced operando X-ray techniques to unveil how MIL-100(Fe) can act as a catalyst for direct methane-to-methanol conversion.

26. Zhang SL, Xie YX, Somerville RJ, Tirani FF, Scopelliti R, Fei ZF, Zhu DR, Dyson PJ: **MOF-based solid-state proton conductors obtained by intertwining protic ionic liquid polymers with MIL-101**. *Small* 2023, **19**:2206999.

27. Zhang J, Zeng YB, Chen LF, Lei XL, Yang YW, Chen ZD, Guo LH, Li L: **A novel core-shell composite of PCN-222@MIPIL for ultrasensitive electrochemical sensing 4-nonylphenol**. *Environ Res* 2023, **225**:115499.

28. Zhao J, Lyu C, Zhang R, Han Y, Wu YD, Wu XL: **Self-cleaning and regenerable nano zero-valent iron modified PCN-224 heterojunction for photo-enhanced radioactive waste reduction**. *J Hazard Mater* 2023, **442**:130018.

29. Yuan S, Qin JS, Xu HQ, Su J, Rossi D, Chen YP, Zhang LL, Lollar C, Wang Q, Jiang HL, Son DH, Xu HY, Huang ZH, Zou XD, Zhou HC: **[TiZrO(COO)] cluster: an ideal inorganic building unit for photoactive metal-organic frameworks**. *Acs Cent Sci* 2018, **4**:105-111.

30. Marks SD, Riascos-Rodriguez K, Arrieta-Pérez RR, Yakovenko AA, Exley J, Evans PG, Hernández-Maldonado AJ: **Lattice expansion and ligand twist during CO adsorption in flexible Cu bipyridine metal-organic frameworks**. *J Mater Chem A* 2020, **8**:18903-18915.

31. • Li MH, Liu YB, Li F, Shen CS, Kaneti YV, Yamauchi Y, Yuliarto B, Chen B, Wang CC: **Defect-rich hierarchical porous UiO-66(Zr) for tunable phosphate removal**. *Environ Sci Technol* 2021, **55**:13209-13218.

Experimental and computational studies show that defects play an important role in not only providing additional sorption sites but also diminishing the sorption energy between MOFs and phosphate.

32. Zhou JJ, Ji WX, Xu L, Yang Y, Wang WQ, Ding HL, Xu XC, Wang WW, Zhang PL, Hua ZL, Chen LY: **Controllable transformation of CoNi-MOF-74 on Ni foam into hierarchical-porous Co(OH)/Ni (OH) micro-rods with ultra-high specific surface area for energy storage**. *Chem Eng J* 2022, **428**:132123.

33. Xiao JD, Li R, Jiang HL: **Metal-organic framework-based photocatalysis for solar fuel production**. *Small Methods* 2023, **7**:2201258.

34. Cao YH, Li X, Yu G, Wang B: **Regulating defective sites for pharmaceuticals selective removal: Structure-dependent adsorption over continuously tunable pores**. *J Hazard Mater* 2023, **442**:130025.

35. Wang SY, Ai ZW, Niu XW, Yang WJ, Kang R, Lin ZY, Waseem A, Jiao L, Jiang HL: **Linker engineering of sandwich-structured metal-organic framework composites for optimized photocatalytic H2 production**. *Adv Mater* 2023,2302512.

36. •• Kirchon A, Feng L, Drake HF, Joseph EA, Zhou HC: **From fundamentals to applications: a toolbox for robust and multifunctional MOF materials**. *Chem Soc Rev* 2018, **47**:8611-8638.

This review covers the fundamentals of the design, engineering, and practical applications of MOFs. The authors also discuss the emerging trends of MOF development, such as multicomponent MOFs, defect development in MOFs, and MOF composites.

37. • Sahayaraj AF, Prabu HJ, Maniraj J, Kannan M, Bharathi M, Diwahar P, Salamon J: **Metal-organic frameworks (MOFs): the next generation of materials for catalysis, gas storage, and separation**. *J Inorg Organomet P* 2023, **33**:1757-1781.

The authors review the synthesis, properties, and application of MOFs in various research fields. The structural adjustability of MOFs is highlighted, and the application potentials in catalysis and other areas are discussed.

38. Ma X, Wang L, Zhang Q, Jiang HL: **Switching on the photocatalysis of metal-organic frameworks by engineering structural defects**. *Angew Chem Int Ed* 2019, **58**:12175-12179.

39. Gao HX, Wang S, Cheong WC, Wang KX, Xu HF, Huang AJ, Ma JG, Li JZ, Ip WF, San Hui K, Dinh DA, Fan X, Bin F, Chen FM, Hui KN: **Topological defect and sp3/sp2 carbon interface derived from ZIF-8 with linker vacancies for oxygen reduction reaction**. *Carbon* 2023, **203**:76-87.

40. Yang H: **A short review on heterojunction photocatalysts: carrier transfer behavior and photocatalytic mechanisms**. *Mater Res Bull* 2021, **142**:111406.

41. Salazar-Marin D, Oza G, Real JA, Cervantes-Uribe A, Perez-Vidal H, Kesarla MK, Torres JG, Godavarthi S: **Distinguishing between type II and S-scheme heterojunction materials: a comprehensive review**. *Appl Surf Sci Adv* 2024, **19**:100536.

42. Wu YL, Qu YN, Su CY, Yang XF, Yang YH, Zhang YN, Huang WH: **Enhanced photoinduced carrier separation in Fe-MOF-525/CdS for photocatalytic hydrogen evolution: improved catalytic dynamics with specific active sites**. *Inorg Chem* 2023, **62**:21290-21298.

43. Liu X, Peng ZH, Lei L, Bi RX, Zhang CR, Luo QX, Liang RP, Qiu JD: **Synergistic effect of photocatalytic U(VI) reduction and chlorpyrifos degradation by bifunctional type-II heterojunction MOF525@BDMTp with high carrier migration performance**. *Appl Catal B Environ Energy* 2024, **342**:123460.

44. Che L, Pan JL, Cai KX, Cong YQ, Lv SW: **The construction of p-n heterojunction for enhancing photocatalytic performance in environmental application: a review**. *Sep Purif Technol* 2023, **315**:123708.

45. Mansingh S, Subudhi S, Sultana S, Swain G, Parida K: **Cerium-based metal-organic framework nanorods nucleated on CeO nanosheets for photocatalytic N fixation and water oxidation**. *Acs Appl Nano Mater* 2021, **4**:9635-9652.

46. Yuan Y, Guo RT, Hong LF, Ji XY, Lin ZD, Li ZS, Pan WG: **A review of metal oxide-based Z-scheme heterojunction photocatalysts: actualities and developments**. *Mater Today Energy* 2021, **21**:100829.

47. • He XY, Ding YJ, Huang ZN, Liu M, Chi MF, Wu ZL, Segre CU, Song CS, Wang X, Guo XW: **Engineering a self-grown TiO/Ti-MOF heterojunction with selectively anchored high-density Pt single-atomic cocatalysts for efficient visible-light-driven hydrogen evolution**. *Angew Chem Int Ed* 2023, **62**:e202217439.

By exploiting the chelating property of ligands and fine control of Ti-BPDC surface reconstruction, the authors synthesize TiO_2/Ti-BPDC-Pt

Z-scheme heterojunctions with selective anchoring of high-density platinum single atoms, which exhibit a high electron-hole separation rate.

48. Fu JW, Xu QL, Low JX, Jiang CJ, Yu JG: **Ultrathin 2D/2D WO/g-CN step-scheme H-production photocatalyst**. *Appl Catal B Environ* 2019, **243**:556-565.

49. •• Xu QL, Zhang LY, Cheng B, Fan JJ, Yu JG: **S-scheme heterojunction photocatalyst**. *Chem Us* 2020, **6**:1543-1559.
The authors discuss the differences of the charge-transfer mechanism between S-scheme, type II, and Z-scheme heterojunctions and highlight current limitations and future development direction.

50. Han XX, Lu BJ, Huang X, Liu C, Chen SX, Chen JW, Zeng ZL, Deng SG, Wang J: **Novel p- and n-type S-scheme heterojunction photocatalyst for boosted CO photoreduction activity**. *Appl Catal B Environ* 2022, **316**:121587.

51. Wang XN, Sayed M, Ruzimuradov O, Zhang JY, Fan YS, Li XX, Bai XJ, Low J: **A review of step-scheme photocatalysts**. *Appl Mater Today* 2022, **29**:101609.

52. Yu WQ, Meng FM, Wei HA, Zhang H, Yao S: **Construction of double Z-scheme Ag3PO4/MOF-In2S3/Bi2S3 heterojunction by micro-Ag bridges for photocatalytic degradation of levofloxacin**. *Appl Surf Sci* 2024, **648**:159010.

53. Yu YZ, Li W, Yang HX, Wei QM, Hou LL, Wu ZL, Jiang YY, Lv CY, Huang YX, Tang JY: **4-Methyl-5-vinyl thiazole modified Ni-MOF/g-CN/CdS composites for efficient photocatalytic hydrogen evolution without precious metal cocatalysts**. *J Colloid Inter Sci* 2023, **651**:221-234.